Optical frequency measurements with the global positioning system: tests with an iodine-stabilized He–Ne laser

Richard W. Fox, Scott A. Diddams, Albrecht Bartels, and Leo Hollberg

Global positioning system- (GPS-) referenced optical frequency combs based on mode-locked lasers offer calibrations for length metrology traceable to international length standards through the SI second and the speed of light. The absolute frequency of an iodine-stabilized He–Ne laser [$^{127}I_2$ $R(127)$ $11-5$ f component] was measured with a femtosecond comb referenced to a multichannel GPS timing receiver. The expected performance and limitations of GPS-referenced comb measurements are discussed.

OCIS codes: 120.3930, 140.7090.

1. Introduction

The global positioning system (GPS) is the primary system for widespread distribution of precise time and frequency signals anywhere on Earth.[1,2] This is accomplished through use of so-called GPS-disciplined oscillators that can combine the low-phase-noise qualities of a good local oscillator with the long-term-frequency accuracy available from the GPS signals, which are steered to international time scales. Through the definition of the speed of light c, there is a direct relation between length and time, and the GPS thus plays a role in the distribution of references for accurate length metrology. As is well known, the accurate measurement of optical frequency has undergone a revolution in recent years with the advent of femtosecond comb technology.[3] However, the fractional-frequency stability and accuracy of femtosecond comb measurements are only as good as the stability and accuracy of the best available rf or optical reference.[4,5] Consequently, it is useful to explore the measurement benefits and limitations of GPS-disciplined oscillator references.

Many of the precision optical frequency measurements performed with femtosecond comb technology in recent years have utilized local cesium standards or hydrogen maser references. In particular, comb frequency measurements of He–Ne lasers stabilized to the f component of the iodine $R(127)$ 11-5 transition have recently been published.[6,7] These measurements employed an optical comb referenced to the known frequency supplied by a Cs-calibrated hydrogen maser. Although hydrogen maser frequency references are widely available at national laboratories and large institutions, they are not commonly found in optical laboratories. Rubidium oscillators are less expensive, more widely available, and offer good short-term performance (low phase noise), but are accurate only to approximately $\Delta f/f \approx \pm 5 \times 10^{-11}$. This is not sufficient, for example, to measure a 633-nm He–Ne laser to better than ± 24 kHz. However, GPS timing receivers are available that steer local oscillators with accuracy derived from a Cs clock ensemble. A number of comb-based optical frequency measurements to date have utilized GPS-disciplined oscillators to reference the combs. The local oscillators include Cs[8] and quartz[9,10] clocks, but little information was provided about the limitations imposed by the GPS. In this paper we discuss measurement accuracies and averaging times that can be expected when GPS-referenced optical frequency combs are used.

We measured the frequency of a commercial I_2-stabilized He–Ne laser[11] [National Institute of Standards and Technology (NIST-126)] using a Ti:sapphire-based femtosecond comb laser referenced to the GPS. We performed the frequency measurement by heterodyning the I_2 He–Ne laser with a single tooth of the comb spectrum around 633 nm and

The authors are with the National Institute of Standards and Technology, 325 Broadway, Boulder, Colorado 80305. R. W. Fox's e-mail address is richard.fox@nist.gov.

Received 11 June 2004; revised manuscript received 10 September 2004; accepted 10 September 2004.

monitoring the beat note with a rf counter. The GPS timing receiver was a commercial unit with a low-phase-noise Rb local oscillator.[12] For measurement durations beyond approximately 10 s, the low-noise local oscillator usually allows more accurate measurements than could be achieved with a standard crystal local oscillator. However, the stability of a GPS-disciplined oscillator at longer averaging times is dependent on the system design and feedback loop performance.[13] Previous experience at NIST with a number of timing receivers has shown that the one-way GPS technique can achieve a typical frequency uncertainty of a few parts in 10^{13} when averaged for 24 h. More accurately known frequency (as precise as $\sim 10^{-15}$) can be obtained from the GPS by use of one of the common-view techniques.[1]

2. Time and Frequency of the Global Positioning System

Over times less than one day, the frequency uncertainty delivered by a GPS timing receiver can vary from unit to unit and is a function of many parameters. These include but are not limited to the number of satellites in view and their geometric arrangement, the algorithms used by the receiver to derive the resultant GPS signal, the time of day, solar activity, and changing delays of the atmospheric propagation. In the very short term ($\sim$1 s) the frequency stability will generally be a function of the type and design of the local oscillator. For longer averaging times the local oscillators are driven to follow the GPS signals with increasingly higher gain, so that beyond approximately 10^3 s the frequency stability and accuracy become increasingly independent of the local oscillator. It is instructive to study the frequency received from the GPS in comparison with a good local clock following Coordinated Universal Time (UTC). Although GPS–UTC is monitored at many locations,[14] one expects this data to be slightly different depending on location, primarily as different satellites would be participating in the measurement and the radio signals may experience different ionospheric delays that are dynamic.[1] GPS–UTC data are available on the Internet in a time-based format for Boulder, Colorado, on the NIST website.[15] Such a data set, spanning one month that includes our He–Ne and comb measurement dates (mid-October to mid-November 2003), is shown in Fig. 1. The data are measurements of the arrival times of 1 pulse/s signals from a GPS unit[16] relative to the UTC (NIST) clock, which is a direct indication of the GPS unit's local oscillator frequency stability. We investigated the frequency stability of the Fig. 1 NIST archive data in two ways: by calculating the overlapping Allan deviation and by differentiating the time data.

The Allan deviation [$\sigma_y(\tau)$] is shown in Fig. 2. At each value of τ, the $\pm 1\sigma$ error bars on the Allan deviation plot indicate the frequency stability that this monitoring station recorded for 68% of the measurement periods that were τ in duration. Of course this is a statistical view of the GPS–UTC stability

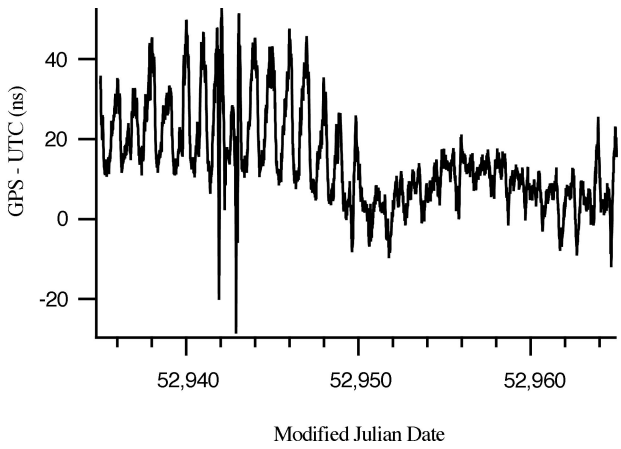

Fig. 1. GPS–UTC time monitoring data for the 30-day period ending at the modified Julian date 52,965.0, or 5 p.m. Mountain Standard Time 21 November 2003. The data are 10-min averages obtained from all the GPS satellites in view from Boulder, Colorado, by use of a typical GPS timing receiver.[16] A diurnal fluctuation (a period of 144 data points) is clearly evident. These data were retrieved from the NIST GPS data archive available on the Internet.[15]

and says little about how unstable or uncertain the frequency was during any particular τ duration. We can look at the frequency stability as a function of time by differentiating the Fig. 1 data and dividing by the time interval between data points. This result, shown in Fig. 3, has a frequency stability of $\Delta f/f \leq \pm 5 \times 10^{-12}$ ($\pm 3\sigma$, 10-min averaging time), although there are obvious excursions to $\Delta f/f = \pm 3 \times 10^{-11}$. These perturbations correspond to a period of intense solar activity that occurred in late October 2003. The right side of Fig. 3 is more representative of nominal GPS frequency stability, and we look at it in more detail in Fig. 4.

The day-to-day fluctuations are somewhat clearer if we study the value of the Allan deviation at one measurement duration, say 1200 s, over a long period of time. In Fig. 5, $\sigma_y(1200\ \text{s})$ as calculated from the

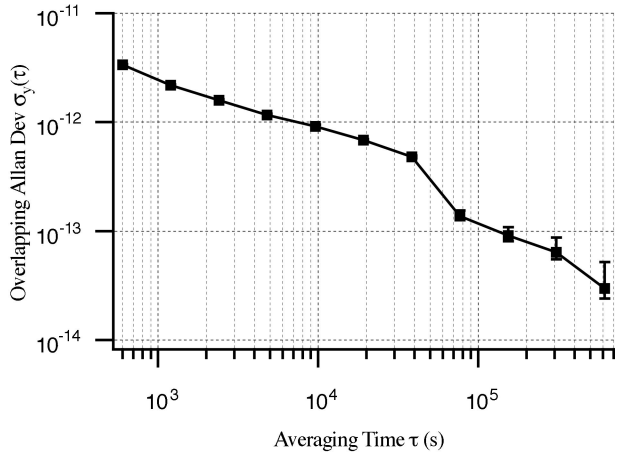

Fig. 2. Frequency stability of the received GPS as calculated from the Fig. 1 data by the overlapping Allan variance routine.

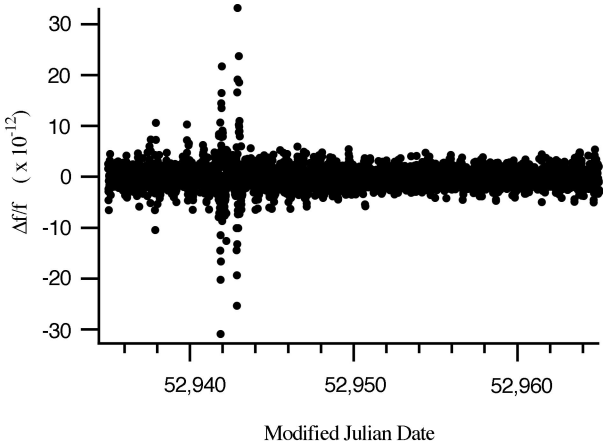

Fig. 3. Frequency stability of the local oscillator that we calculated from the Fig. 1 data by differentiating and dividing by the time interval between data points. The features near modified Julian date 52,942 are associated with a period of intense solar activity in October 2003. The diurnal fluctuation evident in Fig. 1 is buried in the noise. A portion of this data during a normal period near modified Julian date 52,956 is shown in Fig. 4.

daily data is plotted for a four-month period that includes the data from Fig. 1. It is evident that, at least for averaging times of 20 min, the GPS frequency on certain days is less stable than on other days.

From this data we draw a number of conclusions that are pertinent to GPS-referenced optical frequency measurements of stable lasers. When we measure a source that is in the short term more stable than the GPS reference [i.e., $(\Delta v/v)_{\mathrm{GPS}} > (\Delta v/v)_{\mathrm{TEST}}$], such as the I_2-stabilized He–Ne laser, the beat-note statistics will correspond to the GPS reference. To measure the He–Ne laser frequency to ± 1 kHz, for example, would require sufficient averaging to reach $\Delta v/v \leq 2 \times 10^{-12}$. Often a typical GPS-disciplined oscillator will provide this level of stability (and accuracy) in $\Delta t = 2000$ s of averaging. However, the mean value reported must be accompanied by an uncertainty, for example, derived from the measurement data's Allan deviation or total deviation.[17] In practice this means that the measurement duration must be significantly longer than 2000 s to provide enough data to calculate the variance at 2000 s. The measurement duration must be eight times longer ($\Delta = 4.4$ h) if the Allan deviation is employed as a statistical predictor and two times longer ($\Delta t = 1.1$ h) if the total deviation is used. If the GPS reference statistics were stationary, or time invariant, then $\sigma_t(\tau)$ would be known, from prior calibrations, for the full measurement duration. In other words, the 2000-s measurement would yield a mean value accompanied by the known $\sigma_y(2000)$ or a total deviation (2000 s) uncertainty from the GPS reference. It is evident from Fig. 3 that the GPS reference statistics are not stationary, although the largest data fluctuation shown in Fig. 3 does in fact correspond to an exceptional anomaly. It is possible that an Internet-accessible GPS–UTC monitoring station could be used to gauge the relative stability of the GPS frequency on a particular day, thereby allowing the frequency measurement uncertainty to be significantly reduced by reliance on the nominal (usual) measurement GPS receiver statistics. Here we take the approach of using the Allan deviation of the measured data to specify the measurement uncertainty.

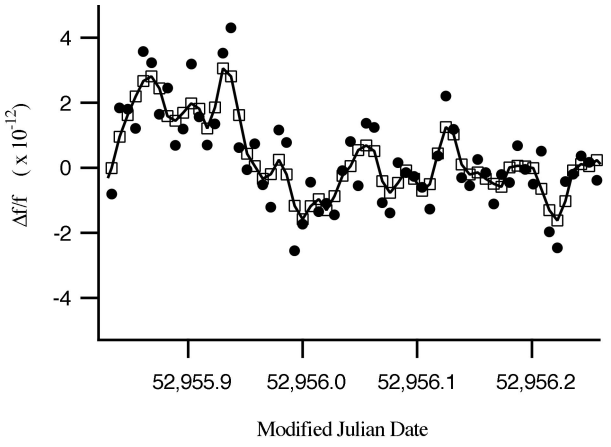

Fig. 4. Ten-hour portion of the Fig. 3 frequency stability data is shown by the filled circles. The open squares are the result of averaging each 10-min data point with the two adjoining neighbors. The curve is therefore an indication of the oscillator's typical frequency stability when averaging for approximately 1800 s (30 min).

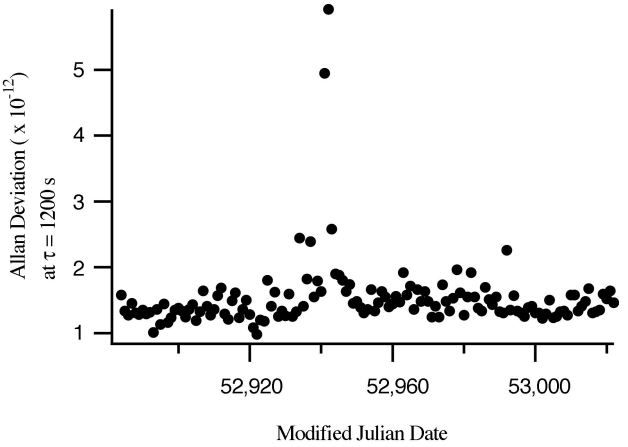

Fig. 5. Allan deviation at 1200 s calculated from the NIST GPS archive data for each day from 2 September 2003 until 18 January 2004. The peak of this plot, on 29 October 2003, corresponds to a period of unusually intense solar activity.

3. Experiment

We phase locked the repetition rate of the mode-locked comb laser[18] ($f_{\mathrm{REP}} \sim 998$ MHz) to a low-phase-noise laboratory synthesizer by controlling the laser's cavity length with a piezoelectric crystal. The synthesizer's reference was a 10-MHz signal supplied by either the GPS timing receiver or in some cases by a hydrogen maser as discussed in Section 4. The hydrogen maser is part of the NIST time scale that is periodically checked against the NIST Cs fountain

clock.[19] Following the commonly used notation, we write the optical frequency of the n^{th} mode of the comb as

$$f_n = \pm f_0 + nf_{\text{REP}}, \quad (1)$$

where n refers to the integer mode index and f_0 refers to the carrier-envelope offset frequency.[20] This is the common frequency offset of all the modes from the harmonics of the repetition rate. We controlled the offset frequency by self-referencing the comb, i.e., by using nonlinear optics to allow different spectral regions of the comb to mix together, forming a heterodyne signal that is referred to as f_0.[21] We then phase locked the frequency f_0 to a known frequency ($f \sim 100$ MHz) from a laboratory synthesizer by acting on the laser comb's pump power. Controlling the two degrees of freedom f_{REP} and f_0, both in the rf range, is sufficient to precisely know the optical frequency of every comb mode.

The iodine laser beam was mixed with the comb output on a beam splitter to provide a heterodyne beat note f_B that we could monitor with a counter. The frequency of the I_2 He–Ne laser can then be written as

$$f_{\text{He-Ne}} = \pm f_0 + nf_{\text{REP}} \pm f_B, \quad (2)$$

where the sign of the beat-note term is positive if the He–Ne frequency is higher than the frequency of the comb mode that is involved. We adjusted the beat-note frequencies to the center of the rf filter bandpass by changing the repetition rate f_{REP}. The correct sign for the frequencies f_0 and f_B in Eq. (2) could also be revealed if we slightly change the respective synthesizer frequencies and note the change in f_B. The only quantity not directly measured in this series of measurements is the integer n, which we can deduce from Eq. (2) (knowing the signs) and with *a priori* knowledge of the He–Ne frequency that is accurate to within $\pm f_{\text{REP}}/2$, or ± 499 MHz.

Each measurement run consisted of our repetitively gating three counters (by a general-purpose interface bus group command) that were monitoring f_0, f_{REP}, and f_B, respectively, each with a 1-s gate time. Extensive tests have previously shown the ability of this femtosecond comb system to measure optical frequencies to the $\Delta v/v \sim 1 \times 10^{-15}$ level when referenced to the NIST time scale.[22,23] An experimental diagram is given in Fig. 6.

We locked the I_2 He–Ne laser to the iodine spectrum (f component) by frequency modulating at 1.1 kHz and 3f detection. The recent International Bureau of Weights and Measures (BIPM) report on realizing the meter stipulates that a modulation width of (6 ± 0.3) MHz should be used to achieve the given relative uncertainty.[24] This value was set (uncertainty ≤ 100 kHz) by observing the He–Ne and comb beat-note envelope with a spectrum analyzer in peak-hold mode. For this modulation width measurement, we suppressed the residual comb jitter caused by

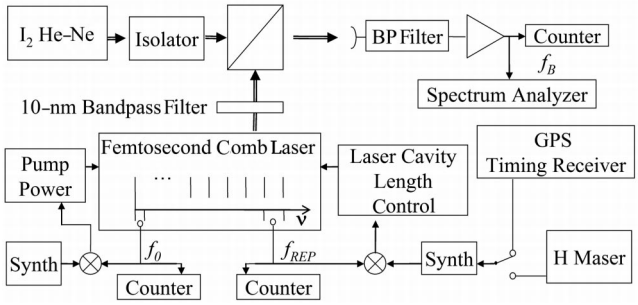

Fig. 6. Measurement system diagram. The comb repetition rate could be referenced to either the GPS receiver or the maser as required. The offset frequency f_0 synthesizer requires no reference since the output is not multiplied by the large factor n. BP, bandpass filter.

our multiplying the 998-MHz frequency reference by $n = 4.7 \times 10^5$ by using a stable optical reference for the repetition rate because even a low-noise maser reference signal results in significant frequency modulation after multiplication to the visible. A beam from a cavity-stabilized laser near $\lambda = 657$ nm was available to serve as a reference, and a comb frequency component was offset phase locked to this red laser by acting on the comb's pump power. This worked well as the reference cavity was well protected from environmental perturbations by a dampening system that included rubber mounts, acoustic shielding, and a vacuum enclosure.

Section 1.7 of the BIPM report gives further stipulations as to the cold-finger temperature, the iodine cell wall temperature, and the one-way intracavity beam power. The cold-finger temperature was 15.03 °C, in accordance with the recommended value of (15.0 ± 0.2)°C. The iodine cell wall temperature in the enclosed laser package was 27.5 °C, within the recommended value of (25 ± 5)°C. The laser optics were cleaned, and then we set the intracavity beam power by monitoring the output power, relying on the manufacturer's stated value of the output coupler transmission of $T = 0.6\%$. We adjusted the output power to 60 μW by rotating the iodine cell. This output power level corresponds to a 10-mW intracavity, within the recommendation of (10 ± 5) mW. The tolerance on the intracavity power recommended by the BIPM report translates to an allowable margin for error of the output coupler transmission of approximately -0.2% to $+0.6\%$.

The He–Ne and comb beat note was detected, bandpass filtered, and amplified to approximately -10 dBm before it was monitored by the counter. A 70-MHz bandpass filter (FWHM ~ 18 MHz) was used, and we centered the signal at 70 MHz by adjusting the comb repetition rate. Approximately 25 μW of the He–Ne light was incident on the photodetector, resulting in a signal-to-noise (S/N) ratio of 25–30 dB in the beat note. Typical signals are shown in Fig. 7. A low-pass filter with a 3-dB cutoff frequency of 90 MHz was used prior to the counter to attenuate the harmonics of the 70-MHz signal caused by amplifier non-

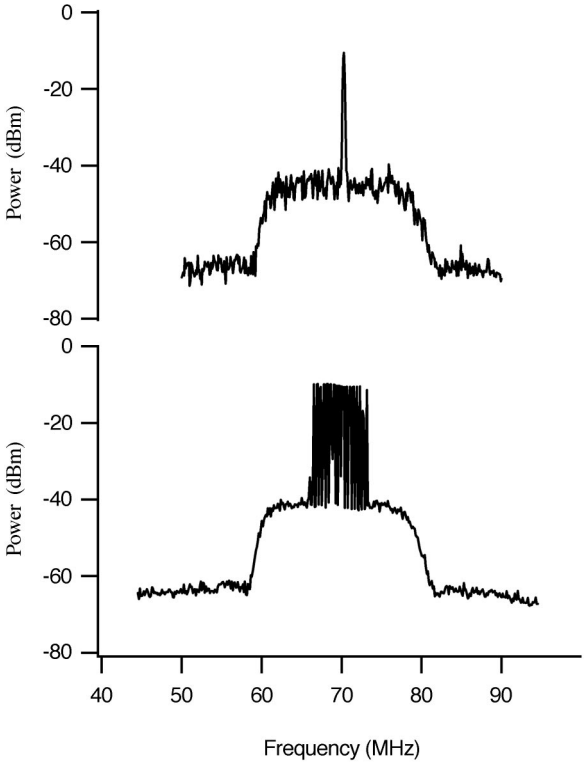

Fig. 7. He–Ne and comb photocurrent beat notes after filtering and amplification, with a 300-kHz resolution bandwidth. The top trace shows a single analyzer sweep of 4-ms duration; the bottom trace is a 100-ms sweep time. The width of the bottom envelope is due to both the He–Ne modulation and the comb jitter.

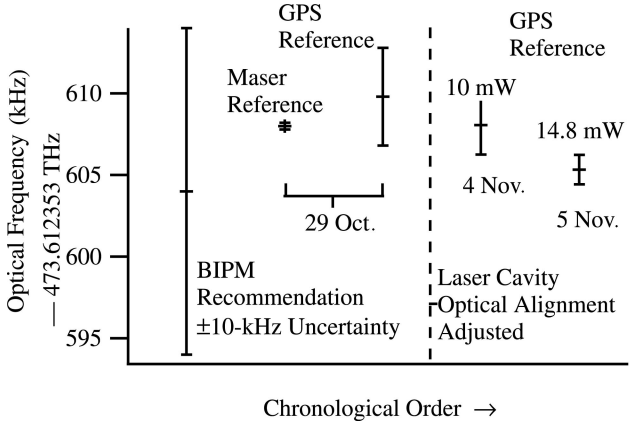

Fig. 8. Summary of the I_2 $R(127)$ 11 − 5 f component frequency measurements. The first two measurements were prior to an optimization of the laser cavity alignment. We increased the laser power between data sets labeled 4 Nov. and 5 Nov. by rotating the iodine cell.

linearities. Several trials were performed to test the sensitivity of the counter to the signal level and to the S/N ratio. We changed the signal level in the range from −1 to −15 dBm by changing the amplification with no apparent change in the counting statistics. Likewise, we reduced the S/N ratio by 5 dB by misaligning the two beams, again with no apparent loss of counts. By no apparent loss of counts we mean that the multiple data runs with these different experimental configurations all produced mean values within the error bars predicted by the Allan deviation.

A 35-dB optical isolator was used at the He–Ne laser output to reduce any spurious backreflection that would disturb the laser frequency. The 3f laser lock error signal was monitored during the beam alignment; and by detuning the isolation to a lower value, we could clearly see the effect of feedback on the error signal. We eliminated the deleterious effects of feedback by making certain that the detector–lens combination was not serving as a retroreflector and that the optical isolator was properly aligned.

4. Frequency Measurements

After ensuring the laser was running within the BIPM recommendations, and studying the signal level and S/N characteristics as described above, we measured the frequency of the $^{127}I_2$-stabilized He–Ne laser as it was locked to the f component of the $R(127)$ 11-5 transition at 632.991 nm. This was done in three separate sets of data over a week's time, each with slightly different conditions as described here. The first data set consisted of one data run with the comb repetition rate phase locked to the NIST hydrogen maser and another with the repetition rate locked to the GPS signal. The second set of data was collected after the laser was optically realigned, and the third set of data was then taken after the intracavity laser power was increased to 14.7 mW. The second and third sets of data were collected with the comb referenced to the GPS signal.

A number of times during each data run, one of the comb laser's phase-locked loops would come out of lock, necessitating a manual relocking. This unlocking occurred because the laser's base plate was not temperature stabilized, and the servo's dynamic range was not sufficient to counteract the thermal drift. As the counters were running asynchronously with the laser electronics, all such dropouts were recorded and removed from the raw data. All the data points from one general-purpose interface bus group trigger were discarded if the offset frequency was different from the nominal value by more than 20 Hz or the repetition rate differed from the set value by more than 0.2 Hz. These are generous limits that served to identify the unlocked condition. The offset and repetition rate data were limited by noise in the counters to approximately $\Delta f/f \approx \pm 5 \times 10^{-11}$ (1σ), or approximately ±50 mHz, at the 1-s gate time.

A summary of the measured frequencies is given in Fig. 8 (and Table 1), along with an indication of the recommended BIPM value. The error bars are derived from Allan deviation calculations and represent different averaging times as discussed below. We performed the optical alignment of the He–Ne laser between the first and second data set by rapidly sweeping the cavity piezoelectric transducer and adjusting one cavity mirror tilt angle alternately in two dimensions. Approximately 5% higher power was ob-

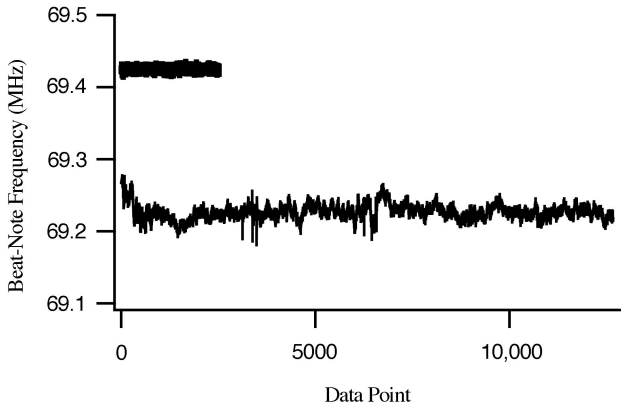

Fig. 9. Counter frequency measurements with 1-s gate times. Data set 1 consisted of two measurements, the comb minus the He–Ne beat note with the comb referenced first to the maser (upper trace) and subsequently referenced to the GPS signal (lower trace). The lower trace is offset by −200 kHz on the graph for clarity.

tained, and the I_2 cell was then slightly rotated to return the output power to the specified values.

The maser-referenced measurement consisted of approximately 2500 data points at a 1-s gate time. The time series and Allan deviation are shown in Figs. 9 and 10, respectively. The data averages down to an uncertainty of $\Delta v/v \leq 3 \times 10^{13}$ at 300 s, or ±200 Hz, as calculated by the Allan deviation. Immediately at the end of this data run the reference of the f_{REP} synthesizer was switched to the GPS timing receiver output. A much longer time series of 12,700 points (1-s gate time) was then collected. Shown as the trace labeled GPS Ref 29 Oct. in Fig. 10, this data averages down to approximately $\Delta v/v = 6 \times 10^{-12}$ at 2000 s, or ±3 kHz. The data trace clearly reaches this level much earlier ($\tau \sim 2$ s), but over this short

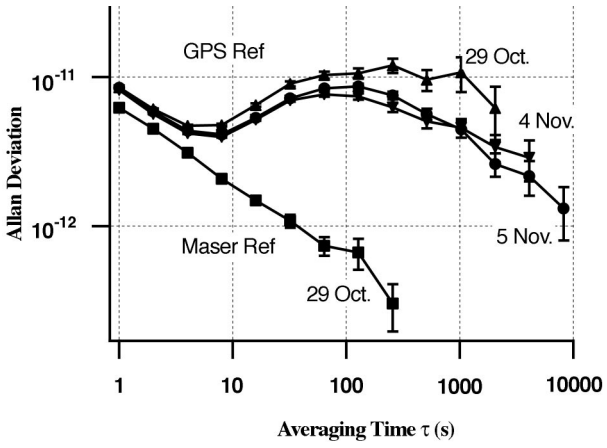

Fig. 10. Filled squares, the Allan deviation of the He–Ne and comb beat note with the comb referenced to the H_2 maser, indicating the intrinsic stability of the I_2 He–Ne laser. Filled circles and triangles, also the He–Ne and comb beat note, but the comb is referenced to the GPS timing receiver signal. The laser optical alignment was adjusted prior to the data labeled 4 Nov. The laser power was increased to 14.8-mW intracavity prior to the data labeled 5 Nov., indicated with filled circles.

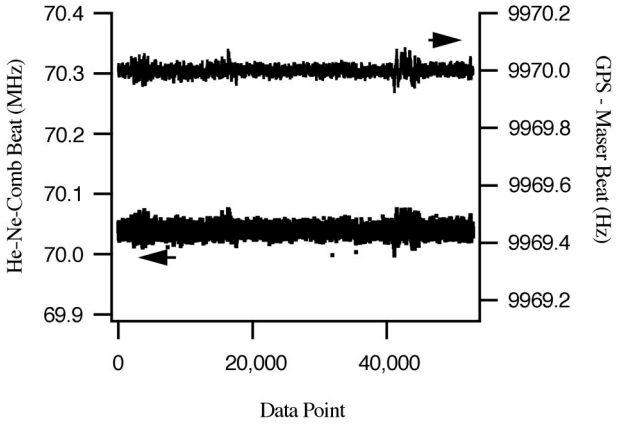

Fig. 11. He–Ne and GPS-referenced comb beat frequency (bottom trace, left axis) and simultaneously the beat between a synthesizer ($f \sim 998$ MHz) referenced to the GPS and a second synthesizer referenced to a maser (top trace, right axis). The data points are 1-s gate-time counts over approximately 14 h. The *Y*-axis scales are adjusted such that $\Delta f_{\mathrm{full\ scale}}/v_0$ are identical. Both data sets exhibit the same Allan deviation for times longer than 20 s. The slightly higher noise level of the He–Ne and comb data corresponds to a slight increase in the Allan deviation at averaging times less than 20 s relative to the GPS-driven Rb oscillator. The obvious correlation of the two time series indicates that in the long term the frequency stability of the GPS is the common limiting factor.

time interval the Rb oscillator frequency is not tightly steered by the GPS signal, and, although stable, it is not necessarily accurate to $\Delta v/v = 6 \times 10^{-12}$. The GPS-steered Rb is controlled for times longer than approximately 100 s, and the Allan plots fall as $\tau^{-1/2}$ reflecting both stability and accuracy.

Following optical realignment of the He–Ne laser, we remeasured the output frequency while also using a fourth counter to monitor the GPS fluctuations relative to the maser. A synthesizer referenced to the maser was offset (by 9970 Hz) from the GPS-referenced f_{REP} signal, and the two synthesizer outputs (the one referenced to the maser and the one tied to GPS) were fed to a double-balanced mixer. The Allan deviation of this He–Ne and GPS data is labeled 4 Nov. in Fig. 10. The Allan deviation of the maser and GPS data is identical for averaging times of 20 s and longer and is not shown. For averaging times less than 20 s, the maser and GPS Allan deviation is slightly less than the He–Ne and GPS data, indicating that on 4 Nov. the He–Ne laser was limiting the stability for very short averaging times rather than the GPS-driven Rb oscillator. The time series of the two data sets are shown in Fig. 11 and are highly correlated. This is a further indication that the long-term behavior of the He–Ne and GPS data is due solely to the GPS frequency stability.

The third and final data set was recorded with the He–Ne laser's intracavity power increased to 14.8 mW. The nominal power shift is approximately −94 Hz/μW of output power, which agrees well with previous data from this laser. The Allan deviation of the data set is labeled as 5 Nov. Fig. 10. We note that the Allan deviation of the first data set is as much as

Table 1. Summary of Optical Frequency Measurements, $\upsilon = \upsilon_R + 473.612353\ \text{THz}\ {}^{127}I_2R(127)\ 11\text{–}5\ f$

Data Set	f_{REP} (Hz)	n	f_0 (MHz)	f_B (Hz)	υ_R (kHz)	$\Delta\upsilon$ (kHz)	Average Time (s)
29 Oct.	998,649,253	474,253	−120	69,424,990	608.0	±0.2	2500
29 Oct.	998,649,253	474,253	−120	69,426,800	609.8	±3	12,700
4 Nov.	998,670,647	474,243	−140	−70,037,173	608.0	±1.8	39,200
5 Nov.	998,670,647	474,243	−140	−70,039,896	605.3	±0.9	52,800

[a] Maser reference.
[b] GPS reference.

twice as high as the second and third sets. The maser and He–Ne 29 Oct. data were taken immediately prior to the first GPS and He–Ne data set and indicate that the He–Ne laser was operating properly and not, for example, suffering from optical feedback. There was a considerable increase in solar storm activity reported on and about this date, and the increased variation of the data is no doubt associated with increased GPS fluctuations as also recorded by the NIST archive (see Figs. 1 and 3).

Table 1 summarizes the optical frequency measurements and displays all the parameters from Eq. (2) for each data set. The measured optical frequency in each case is $\upsilon = 473.612353\ \text{THz} + \upsilon_R$. The repetition rate f_{REP} and offset frequency f_0 are 12-digit synthesizer settings. f_B is the beat-note mean in the given averaging time. The negative signs were deduced from the change in f_B with changes to f_{REP} and f_0. The first three measurements (29 Oct.[a,b] and 4 Nov.) are with the laser at 10-mW intracavity power. The final data, 5 Nov. is with 14.8-mW intracavity power. The uncertainty $\Delta\upsilon$ corresponds to the Allan deviation (Fig. 10) at the given averaging time, i.e. $\Delta\upsilon = \upsilon \times \sigma(\tau)$. The measured frequencies are well within the ±10-kHz uncertainty bounds of the BIPM recommended value.

We note that the GPS timing receiver used here did not have the capability to accept position coordinates as input. The unit was tested with the antenna located near the antenna used for the NIST archive GPS receiver. This is a surveyed location, and the elevation reported by the GPS receiver under test was 19 m too high, which may have led to higher medium-term frequency fluctuations than would otherwise have been the case. In this test, conducted in January 2004, the unit's timing output was monitored for three days with a time-interval analyzer referenced to the NIST 10-MHz maser signal. Subsequently we downloaded the NIST GPS archive data for the same period for comparison. The Allan deviation of the test unit data was approximately three to four times higher than the NIST archive for averaging times in the $10^3 - 10^4$-s range. At longer times the two Allan deviations converge. This is consistent with the earlier observation that a GPS-disciplined oscillator's stability depends on system design and feedback loop performance.

5. Conclusions

We have calibrated an iodine-stabilized He–Ne laser in a measurement traceable to SI units by employing a multiple-satellite GPS timing receiver as the frequency reference for a femtosecond comb. For averaging times $\tau \geq 1$ s, an uncertainty of $\Delta\upsilon/\upsilon \leq 1 \times 10^{-11}$ (±5 kHz) was attainable with our GPS receiver, even on a rather noisy day for the GPS system. Although the He–Ne stability (as evidenced by maser-referenced measurements) was approximately $6 \times 10^{-12}\,\tau^{-1/2}$ out to at least 250 s, with the GPS receiver as a reference, approximately 66 min of averaging were required to reach a measurement uncertainty of ±1 kHz [i.e., with the Allan variance as a predictor, $\sigma_y(4000\ \text{s})$ indicates an uncertainty of ±1 kHz after 32,000 s of data]. For times longer than a few hundred seconds the GPS-referenced comb to He–Ne beat notes typically followed a slope proportional to $\tau^{-1/2}$, although this was not constant day to day during the period of these experiments. It is likely that different receivers will exhibit slightly different averaging statistics.

We acknowledge the NIST Manufacturing Engineering Laboratory for funding this research. We thank D. Howe, M. Lombardi, and A. Novick for helpful discussions and V. Zhang and T. Parker for testing the GPS timing receiver versus UTC–NIST. Mention of products in this paper does not imply recommendation or endorsement by the National Institute of Standards and Technology.

References and Notes

1. J. Levine, "Time and frequency distribution using satellites," Rep. Prog. Phys. **65,** 1119–1164 (2002).
2. M. A. Lombardi, L. M. Nelson, A. N. Novick, and V. S. Zhang, "Time and frequency measurements using the global positioning system," Cal. Lab. Int. J. Metrol. (Sept.) 26–33 (2001).
3. Th. Udem, R. Holzwarth, and T. W. Hänsch, "Optical frequency metrology," Nature (London) **416,** 233–237 (2002).
4. S. A. Diddams, D. J. Jones, J. Ye, S. T. Cundiff, J. L. Hall, J. K. Ranka, R. S. Windeler, R. Holzwarth, Th. Udem, and T. W. Hänsch, "Direct link between microwave and optical frequencies with a 300 THz femtosecond laser comb," Phys. Rev. Lett. **84,** 5102–5105 (2000).
5. J. L. Hall and J. Ye, "Optical frequency standards and measurement," IEEE Trans. Instrum. Meas. **52,** 227–231 (2003).
6. S. N. Lea, W. R. C. Rowley, H. S. Margolis, G. P. Barwood, G. Huang, P. Gill, J.-M. Chartier, and R. S. Windeler, "Absolute frequency measurements of 633 nm iodine-stabilized helium-neon lasers," Metrologia **40,** 84–88 (2003).
7. L.-S. Ma, M. Zucco, S. Picard, L. Robertsson, and R. S. Windeler, "A new method to determine the absolute mode number of a mode-locked femtosecond-laser comb used for absolute optical frequency measurements," IEEE J. Sel. Top. Quantum Electron. **9,** 1066–1071 (2003).

8. R. Holzwarth, A. Yu. Nevsky, M. Zimmermann, Th. Udem, T. W. Hänsch, J. Von Zanthier, H. Walther, J. C. Knight, W. J. Wadsworth, P. St. J. Russell, M. N. Skvortsov, and S. N. Bagayev, "Absolute frequency measurement of iodine lines with a femtosecond optical synthesizer," Appl. Phys. B **73,** 269–271 (2001).
9. G. Ferrari, P. Cancio, R. Drullinger, G. Giusfredi, N. Poli, M. Prevedelli, C. Toninelli, and G. M. Tino, "Precision frequency measurement of visible intercombination lines of strontium," Phys. Rev. Lett. **91,** 243002 (2003).
10. P. Cancio Pastor, G. Giusfredi, P. De Natale, G. Hagel, C. de Mauro, and M. Inguscio, "Absolute frequency measurements of the $2^3S_1 \rightarrow 2^3P_{0,1,2}$ atomic helium transitions around 1083 nm," Phys. Rev. Lett. **92,** 023001 (2004).
11. Winters Electro-Optics Inc. Model 100.
12. Symmetricom XLI.
13. J. A. Davis and J. M. Furlong, "Report on the study to determine the suitability of GPS disciplined oscillators as time and frequency standards traceable to the UK National Time Scale UTC(NPL)," NPL Rep. CTM 1 (National Physical Laboratory, Teddington, Middlesex, UK, 1997).
14. UTC–GPS time is monitored in Paris and disseminated monthly through the BIPM Circular T.
15. http://www.boulder.nist.gov/timefreq/service/gpstrace.htm.
16. The NIST archive GPS receiver is a Motorola Oncore unit.
17. C. A. Greenhall, D. A. Howe, and D. B. Percival, "Total variance, an estimator of long-term frequency stability," IEEE Trans. Ultrason. Ferroelectr. Freq. Control **46,** 1183–1191 (1999).
18. A. Bartels and H. Kurtz, "Generation of a broadband continuum by a Ti:sapphire femtosecond oscillator with a 1-GHz repetition rate," Opt. Lett. **27,** 1839–1841 (2002).
19. S. R. Jefferts, J. Shirley, T. E. Parker, T. P. Heavner, D. M. Meekhof, C. Nelson, F. Levi, G. Costanzo, A. De Marchi, R. Drullinger, L. Hollberg, W. D. Lee, and F. L. Walls, "Accuracy evaluation of NIST-F1," Metrologia **39,** 321–336 (2002).
20. J. Reichert, R. Holzwarth, Th. Udem, and T. W. Hänsch, "Measuring the frequency of light with mode-locked lasers," Opt. Commun. **172,** 59–68 (1999).
21. T. M. Ramond, S. A. Diddams, L. Hollberg, and A. Bartels, "Phase-coherent link from optical to microwave frequencies by means of the broadband continuum from a 1-GHz Ti:sapphire femtosecond oscillator," Opt. Lett. **27,** 1842–1844 (2002).
22. S. Bize, S. A. Diddams, U. Tanaka, C. E. Tanner, W. H. Oskay, R. E. Drullinger, T. E. Parker, T. P. Heavner, S. R. Jefferts, L. Hollberg, W. M. Itano, and J. C. Bergquist, "Testing the stability of fundamental constants with the $^{199}Hg^+$ single-ion optical clock," Phys. Rev. Lett. **90,** 150802 (2003).
23. L. Hollberg, C. W. Oates, E. A. Curtis, E. N. Ivanov, S. A. Diddams, Th. Udem, H. G. Robinson, J. C. Bergquist, R. J. Rafac, W. M. Itano, R. E. Drullinger, and D. J. Wineland, "Optical frequency standards and measurements," IEEE J. Quantum Electron. **37,** 1502–1513 (2001).
24. T. J. Quinn, "Practical realization of the definition of the metre, including recommended radiations of other optical frequency standards (2001)," Metrologia **40,** 103–133 (2003).